「高度DFC-PowerChipに向けたレーザ描画の開発（項目⑦⑱）」

> 40 MW unstable cavity microchip laser for laser writing

Hwan Hong LIM

Division of Research Innovation and Collaboration

Institute for Molecular Science (IMS)

Outline

1. Overview of fs-laser micromachined waveguide
2. Record peak power microchip laser with unstable cavity
3. Summary

fs-laser micromachined waveguides

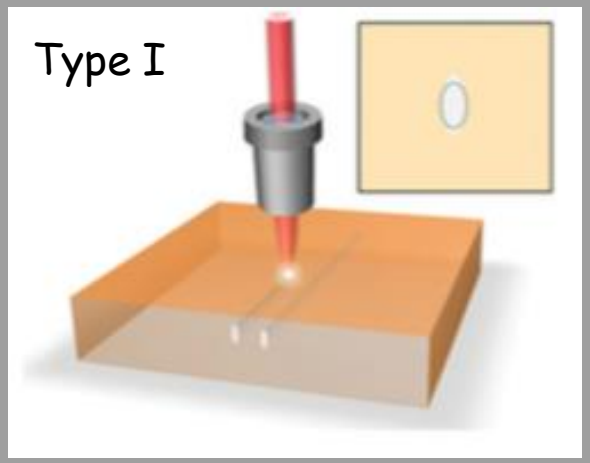

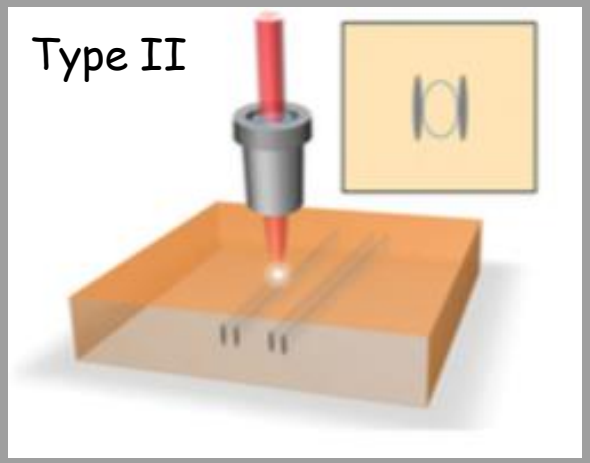

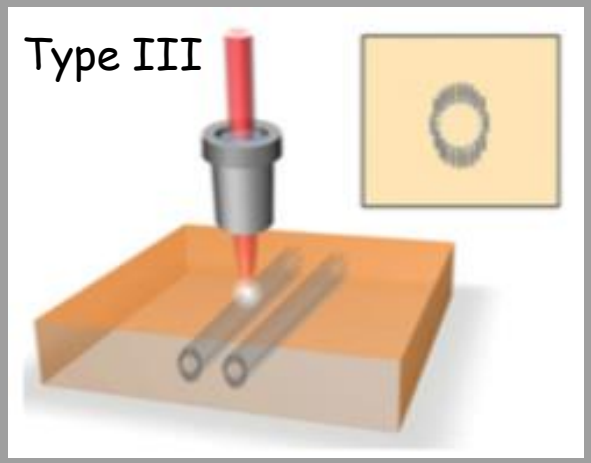

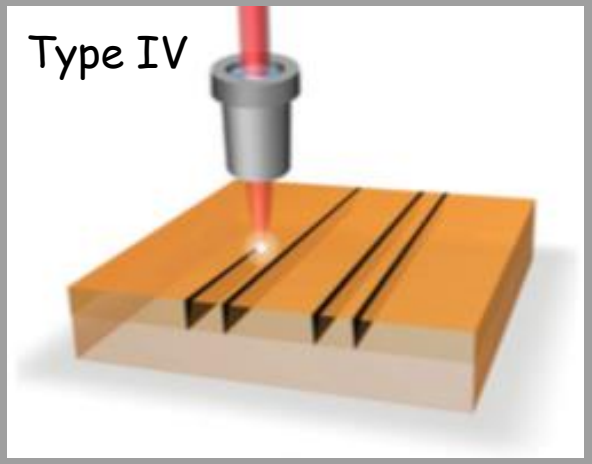

- Mechanism:
  - Strong field ionization (MPI, TI)
  - a hot and dense electronic plasma, and a lattice of ions
  - Ultra fast ablation by Coulomb explosion (electrons and ions ejection)
- Laser parameters (w_0, τ, E, f)
- Material properties (E_g, W, κ, GVD)

Ref. F. Chen and J. R. Vazquez de Aldana, Laser Photonics Rev. **8**, 251-275 (2014).

Type I : Directly written waveguides

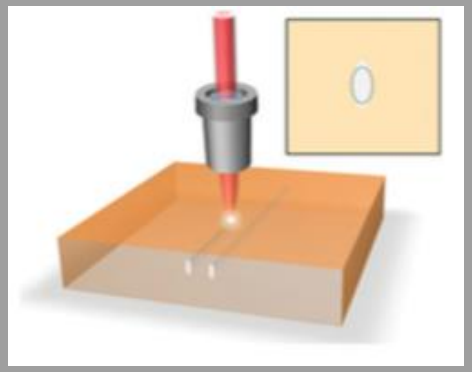

LN, ~0.2 μJ, ~100 fs

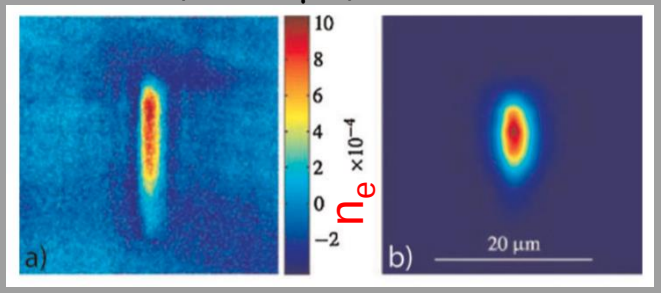

Appl. Phys. A 89, 127 (2007).

- $\Delta n > 0$ in the focal volume → the waveguide core
  - Positive change is very common in amorphous materials, e.g., in most glasses.
  - A few crystals (LN, Nd:YCOB and ZnSe) were used for Type I waveguide.
- Weak damage or modification
  - Point defect creation for LN → lower spontaneous polarization
- Advantages
  - Ease 3D fabrication
- Disadvantages
  - Degradation of bulk related properties in the core due to the even weak damage (NLO coefficient, PL, …)
  - Unstable or removed under high temperature, not suitable for high-power applications
  - Light polarization sensitive guiding

Type II : Stress induced waveguides

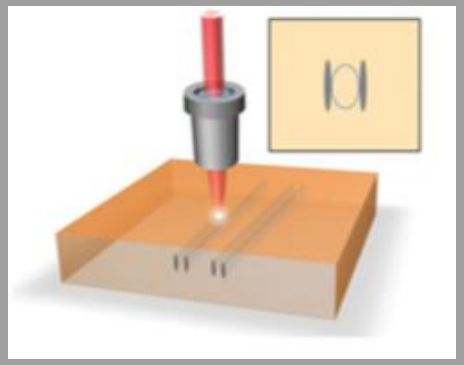

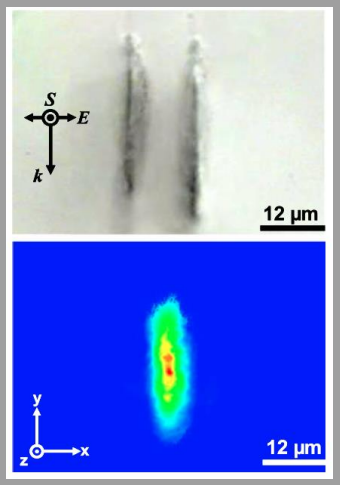

- The waveguides are in the vicinal region of the fs-laser induced tracks.
- $\Delta n < 0$ in the focal volume due to expansion of the lattices → a relatively high index in the vicinal surrounding regions by stress-induced effects.
- Advantages
  - Preservation of luminescence and nonlinear properties of the bulk.
  - Both TM, TE guiding is possible in some crystals.
  - Very stable waveguide at high temperature, suitable for high power operation.

Type II : Stress induced waveguides

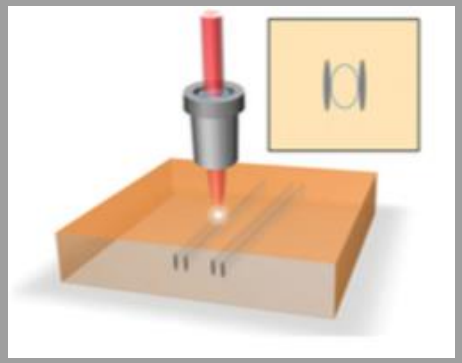

x-cut LN, ~0.3 μJ, ~ 1.2 ps, 100 kHz, 1 mm/s.

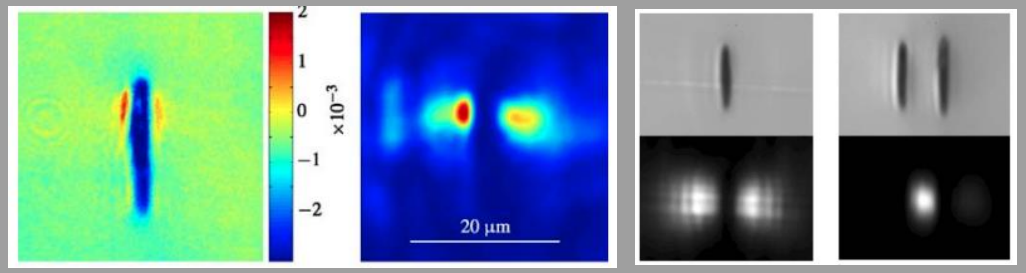

Appl. Phys. A 89, 127 (2007).

Nd(2 at.%):YAG ceramic
(Baikowski Japan),
~0.8 μJ, ~ 120 fs, 1 kHz, 50 μm/s.

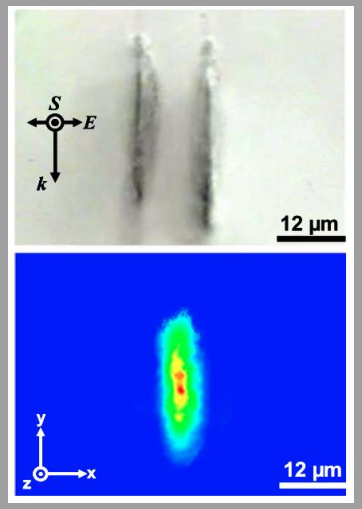

Appl. Phys. B 95, 85 (2009).

Nd(2 at.%):YAG ceramic (Baikowski Japan),
~4 J/cm^2, ~ 120 fs, 1 kHz, 25 μm/s.

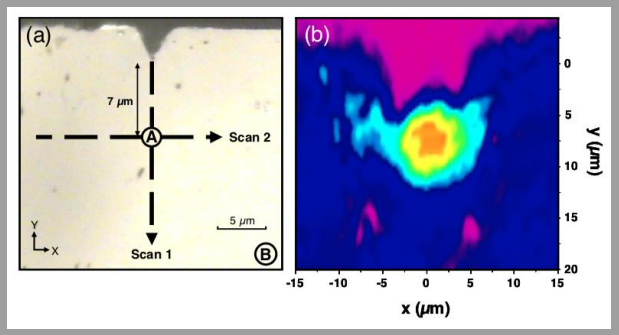

Opt. Express 15, 13266 (2007).

α-quartz ([001]//k),
~14 μJ, ~ 120 fs, 1 kHz, <1 mm/s.

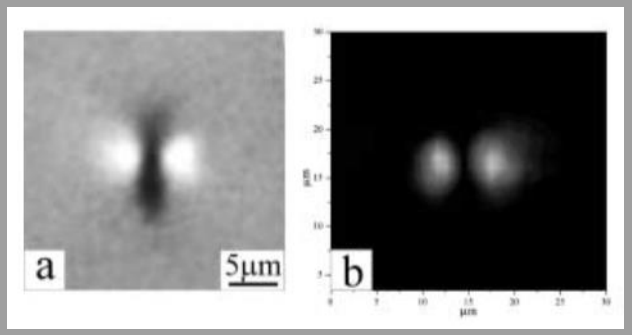

Appl. Phys. A 76, 309 (2003).

Type III : Depressed cladding waveguides

PPMgSLT, ~0.4 μJ, 300 fs

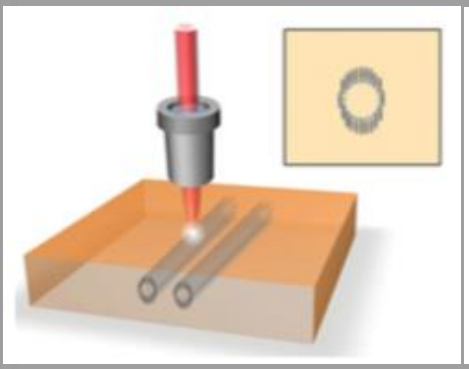

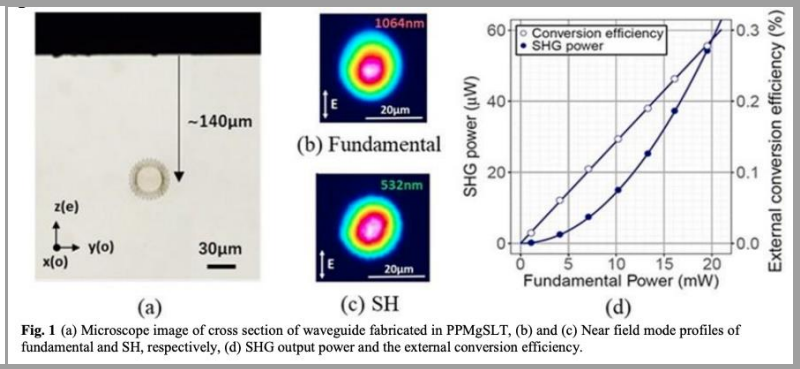

Fig. 1 (a) Microscope image of cross section of waveguide fabricated in PPMgSLT, (b) and (c) Near field mode profiles of fundamental and SH, respectively, (d) SHG output power and the external conversion efficiency.

OXIDE Co. CLEO_Europe (2019).

Nd:YAG ceramic , <0.4 μJ, 120 fs, 1 kHz, 0.7 mm/s

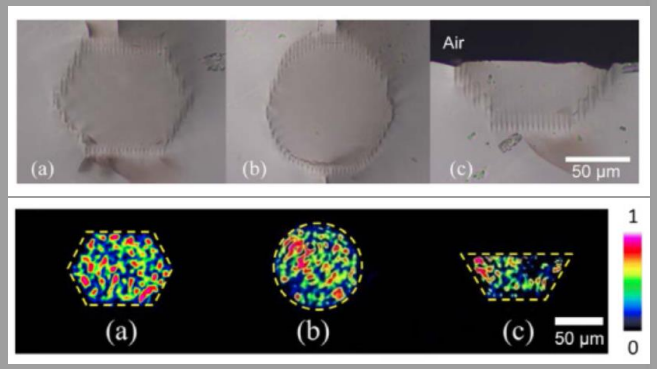

Opt. Express 20, 18620 (2012).

- Similar to Type II, $\Delta n < 0$ in the focal volume. The waveguide consists of a core surrounded by a number of low-index tracks. Those tracks are close to each other (few micrometers), constructing a quasicontinuous low-index potential barrier wall, which allows the confinement of the light field inside.

- Advantages
  - Designable waveguide cross section shape and size.
  - Circular cross section is suitable for fiber-waveguide-fiber integrated photonic system.

Type IV : Ablated ridge waveguides

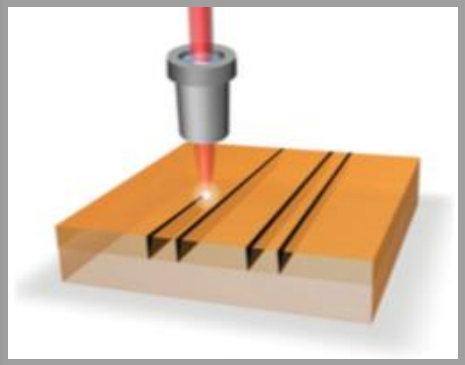

Nd:YAG crystal, 2.1 μJ, ~50 J/cm^2, 120 fs, 1 kHz, 50 μm/s

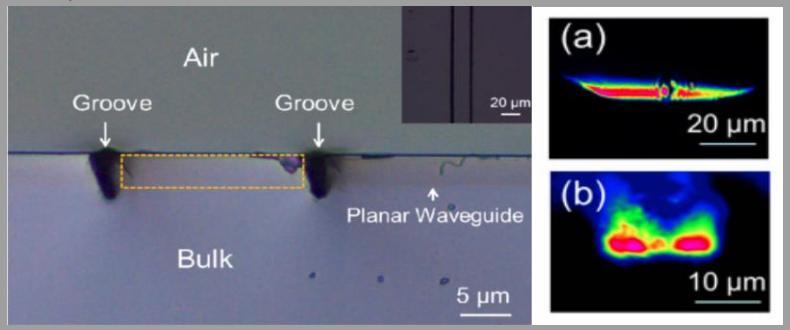

Opt. Mat. Express 2, 657 18620 (2012).

x-cut $LiNbO_3$, <0.3 μJ, 120 fs, 1 kHz, 0.5 mm/s, for mid-IR wavelength

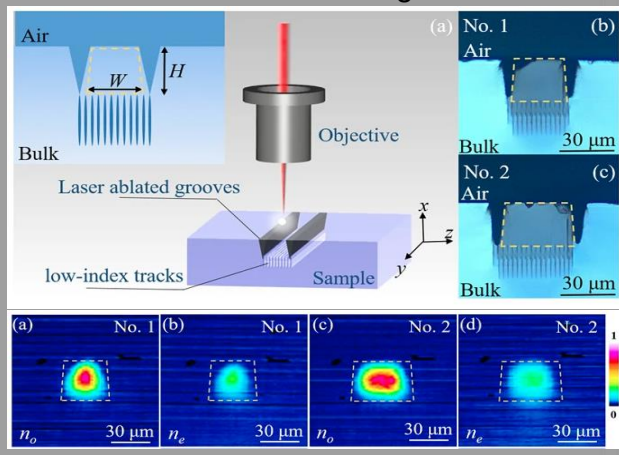

Sci. Rep. 7, 7034 18620 (2017).

- High intensity fs pulse induced ablation.
- Construction of ridge waveguide on planar waveguide substrates.
- All laser machined ridge waveguide (Type III + IV).
- Disadvantage
  - Rough side wall by ablation (Loss of >> 3 dB/cm)
  - A postablation treatment such as ion-beam sputtering or HF etching may be required to reduce the roughness of the ablated air gaps.

Pulse width dependence of laser induced breakdown

Laser
(τ, ω)

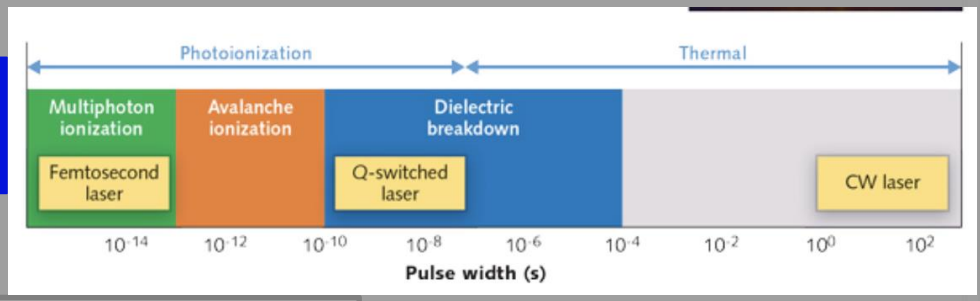

Material

- Thermal explosion model
- Thermal lensing
- …

ΔT

Plasma

- Impact cascade (avalanche) ionization
- Photon ionization
- Kerr lensing for filamentation
- …

Phase transition / breakdown (damage)

Damage on a dielectric coating

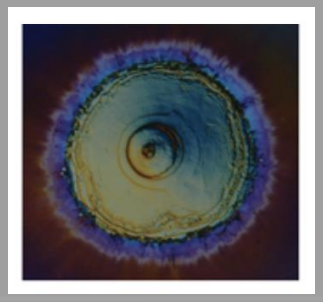

Drilling in steel foils

fs laser ps ns

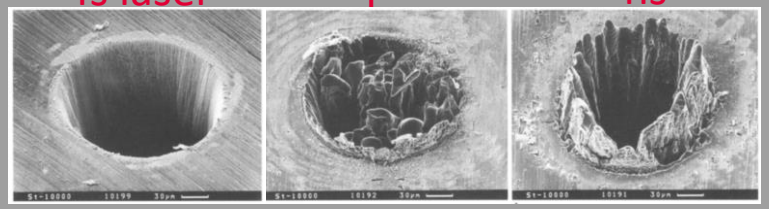

Gas-lighter ignition using laser induced air-breakdown spark

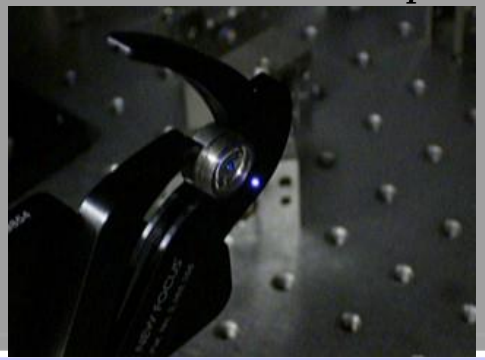

Pulse width dependent breakdown threshold

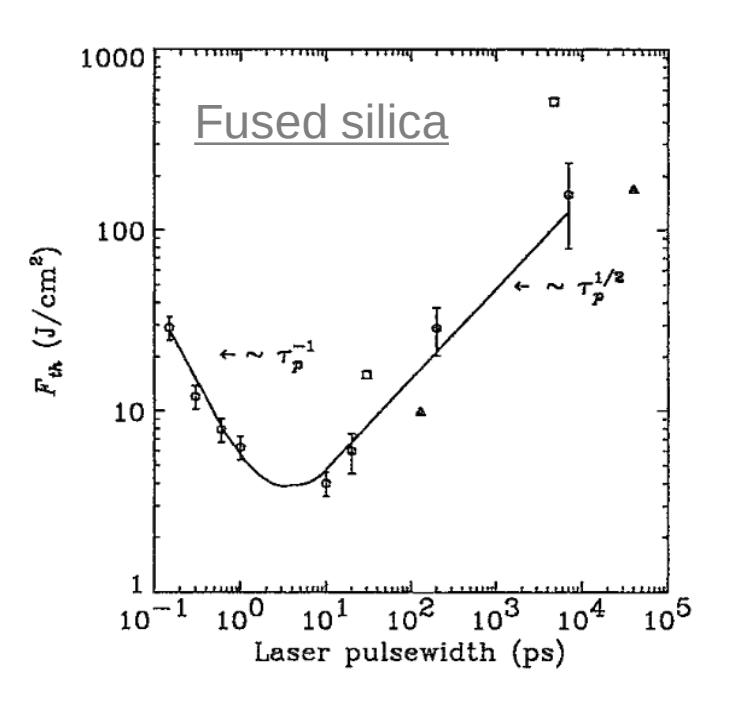

D. Du, et al., Appl. Phys. Lett. **64**, 3071 (1994).

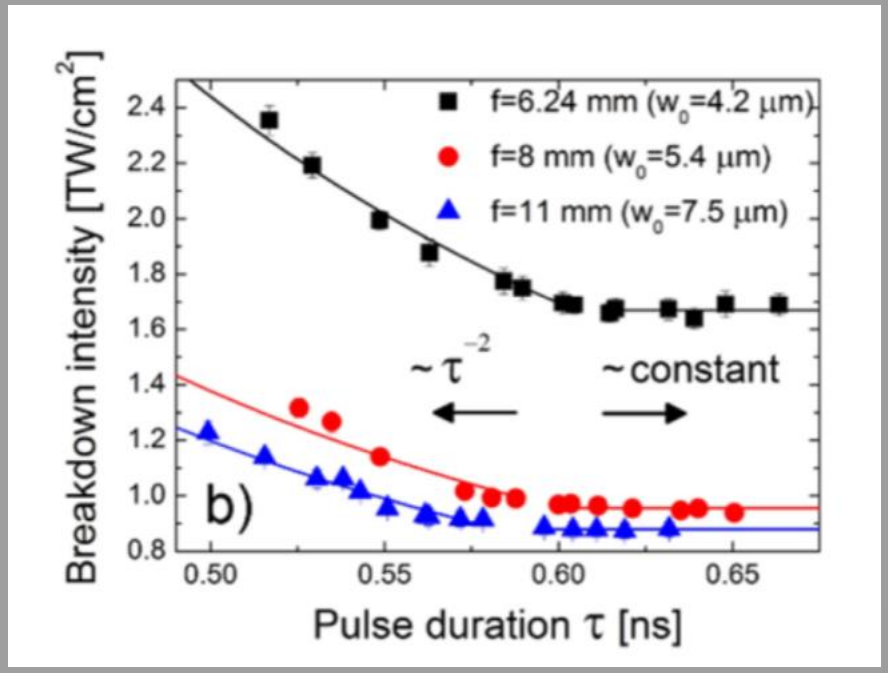

H. H. Lim and T. Taira, Opt. Express **25**, 6302 (2017).

Pulse width dependent laser-induced periodic surface structure (LIPSS)

(a) T = 450 fs	(b) T = 500 ps	(c) T = 1 ns	(d) T = 2.5 ns
N = 1666	N = 500		
1 μJ/pulse	1 mJ/pulse		
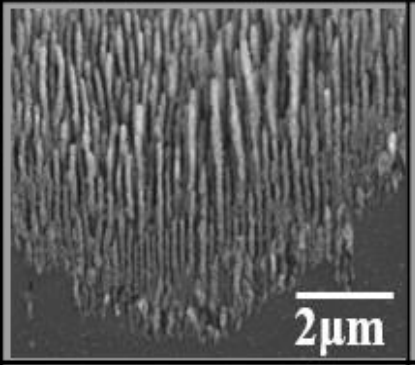	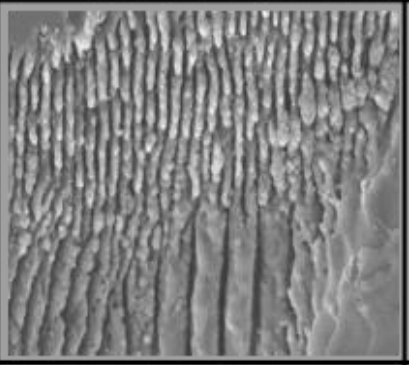	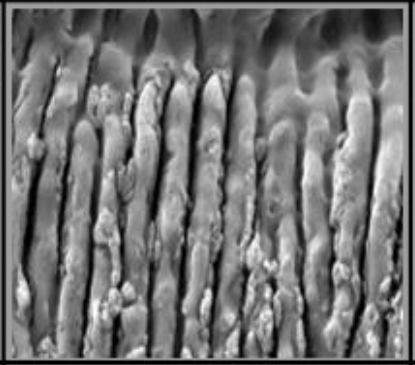	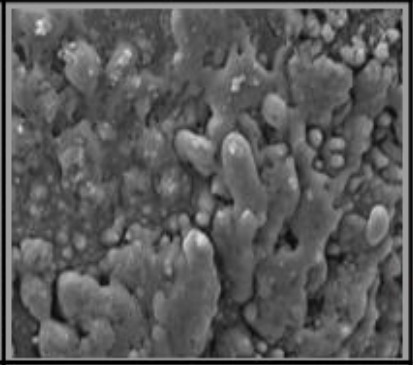
HSFL	HSFL and LSFL	LSFL	-

Surface SEM images of LIPSS on 6H-SiC. T= (a) 450 fs, (b) 500 ps, (c) 1 ns and (d) 2.5 ns

Ref. R. Miyagawa, T. Taira, et al., LIC 2019, LIC6-5.

Outline

1. Overview of fs-laser micromachined waveguide

2. Record peak power microchip laser with unstable cavity

3. Summary

Problems of brightness scale for flat-flat cavity MCL

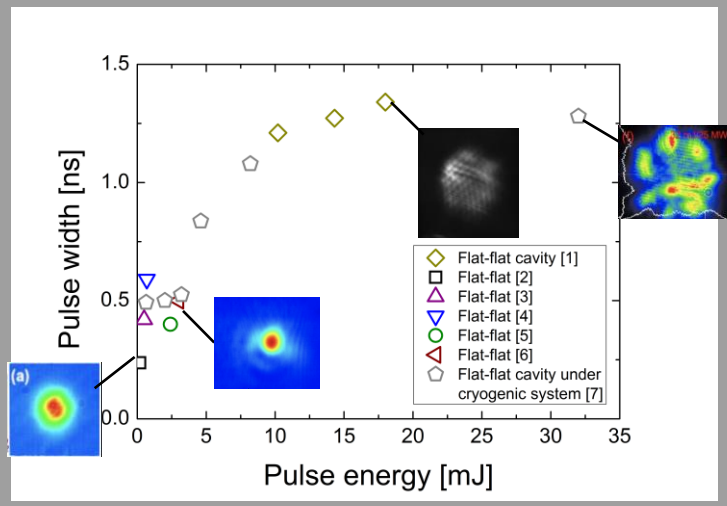

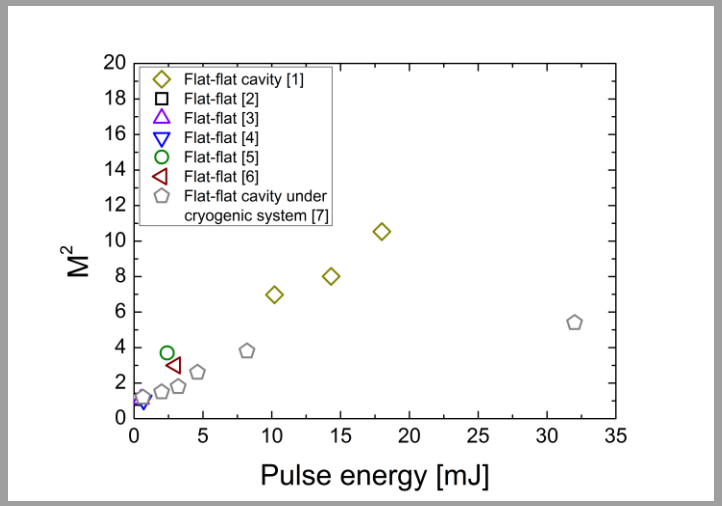

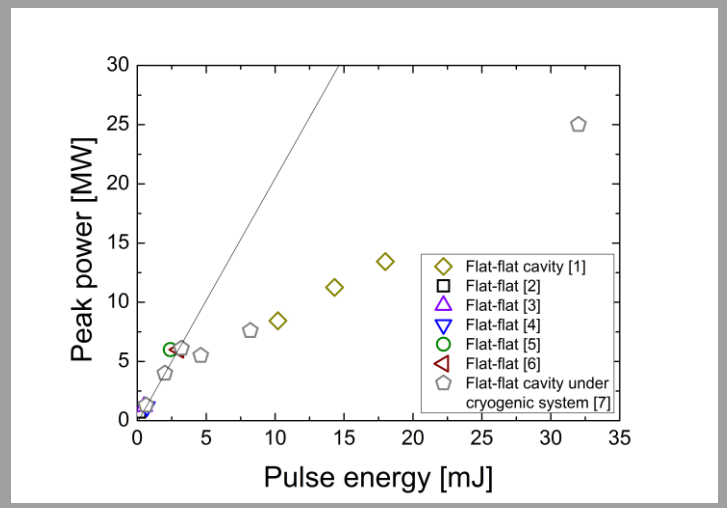

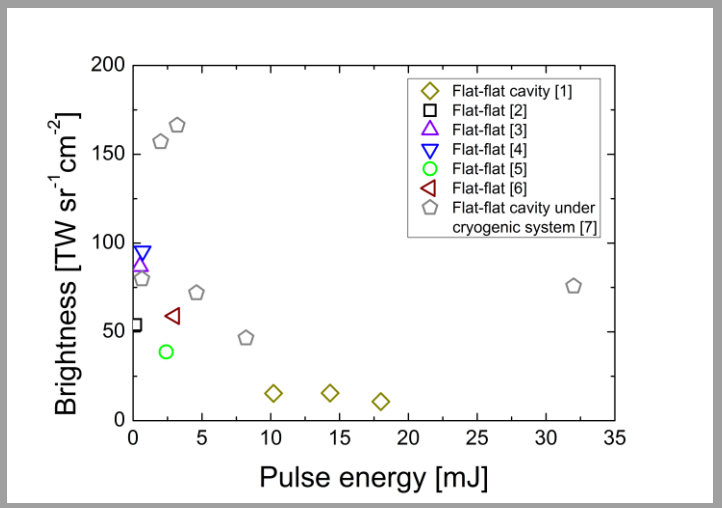

[1] H. H. Lim and T. Taira, Opt. Express **27**, 31307 (2019).
[2] J. Dong, et al., Opt. Express **15**, 14516 (2007).
[3] A. Agnesi, et al., Appl. Phys. Lett. **89**, 101120 (2006).
[4] H. Sakai, T. Taira, et al., Opt. Express **16**, 19891 (2008).
[5] N. Pavel, T. Taira, et al., Opt. Express **19**, 9378 (201
[6] H. H. Lim and T. Taira, Opt. Express **25**, 6302 (2017
[7] X. Guo, et al., Opt. Express **27**, 45 (2019).

Unstable cavity MCL for brightness scaling

- Wider and controllable mode volumes
- Uniform beam pattern of doughnut shape
  - No beam pattern degradation for energy scaling
- A good focusability of doughnut beam as a Bessel-like beam

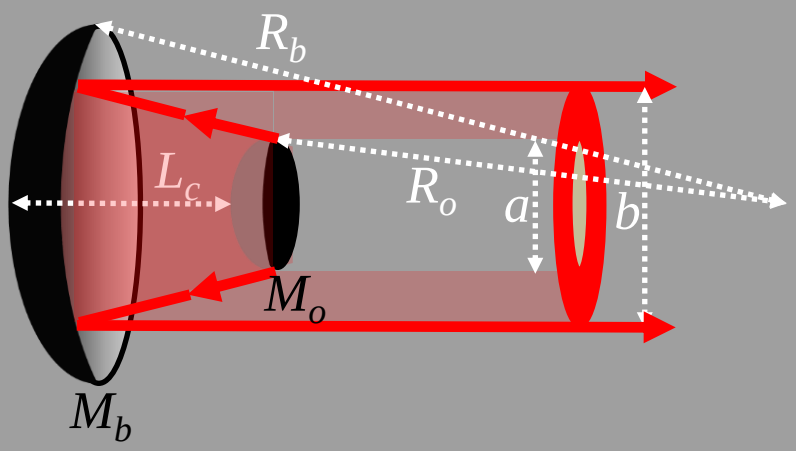

Positive branch confocal cavity

$$m = \frac{b}{a} = -\frac{R_b}{R_o}$$

$$R_b = \frac{2\,mL_c}{m-1}$$

$$R_o = -\frac{2\,L_c}{m-1}$$

$m = \sqrt{2}$

$m = 2$

$m = 3$

Experimental setup I : flat-convex cavity

Microchip laser with unstable cavity

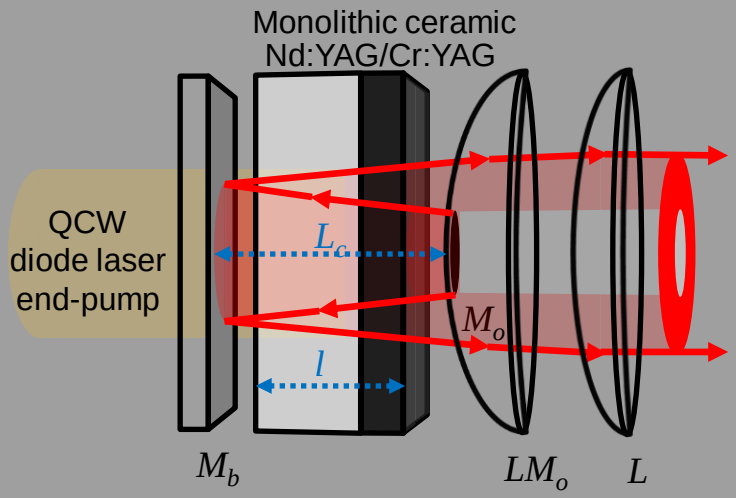

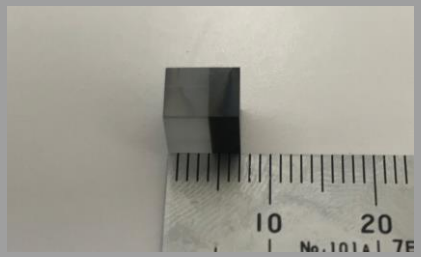

- 700 W pump diode @ 808 nm, 10 Hz during <400 μs
- Monolithic ceramic with a dimension of 6 X 6 X 7(l) mm^3
- 1.1 at.% Nd^{3+} doping and 30% of initial transmittance of Cr^{4+}:YAG

- Flat back cavity mirror M_b
- A half inch plano-convex lens LM_0 with a radius of curvature of 52 mm (for m of $\sqrt{2}$ for the confocal cavity)
- Output coupler (OC) M_0, HR coated on the center part of LM_0 in a spot diameter of 2 mm
- Collimation lens L with a focal length of 50~150 mm in case of the lens position

H. H. Lim and T. Taira, Opt. Express **27**, 31307 (2019).

Laser characteristics

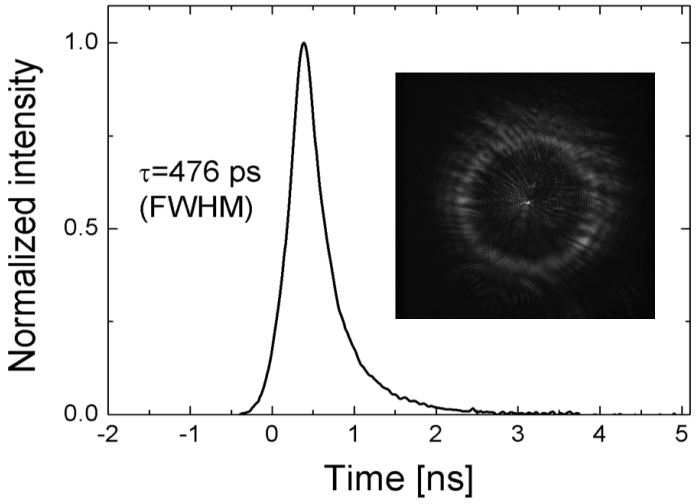

- Doughnut beam pattern with a center Poisson spot
- Pulse energy of 13.2 mJ @ 10 Hz
- Pulse width of 476 ps
  - Record peak power of 27.7 MW

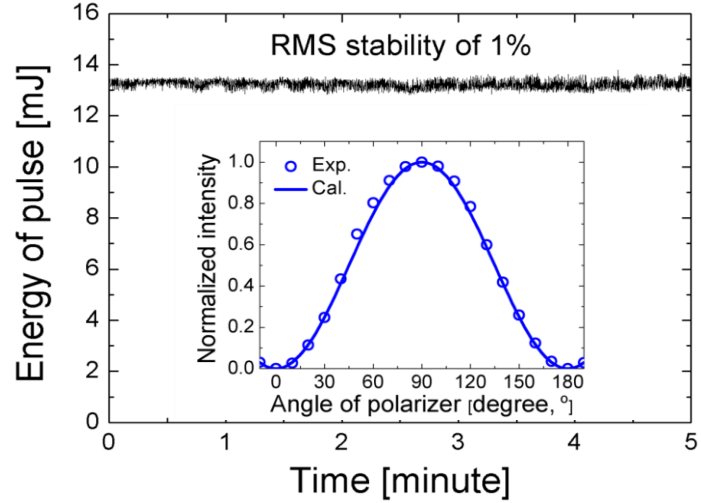

- Short term RMS stability <1%
- Linear polarization @ 10 Hz
  (may be pump power induced birefringence and depolarization due to stress and heat)
  - The polarization ratio $P = \frac{I_{max} - I_{min}}{I_{max} + I_{min}} = 0.997$

H. H. Lim and T. Taira, Opt. Express **27**, 31307 (2019).

Beam quality and pattern

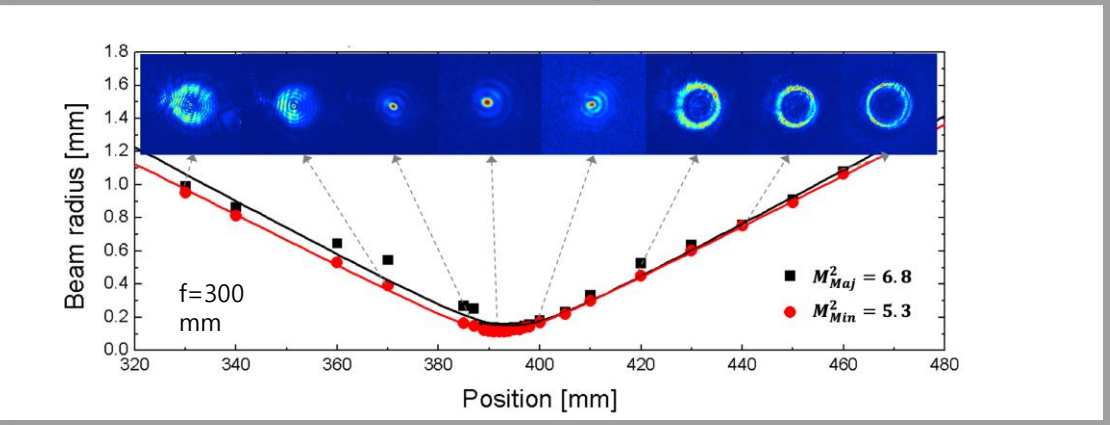

- M^2 $(M^2_{pc}) = 6$ (5.8) , second-moment based M^2 and 86.5% power-content based M^2_{pc} $\quad M^2_{ave} = \sqrt{M^2_{maj} M^2_{min}}$
- Bessel-like beam at focal point

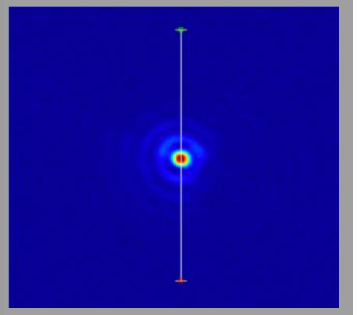

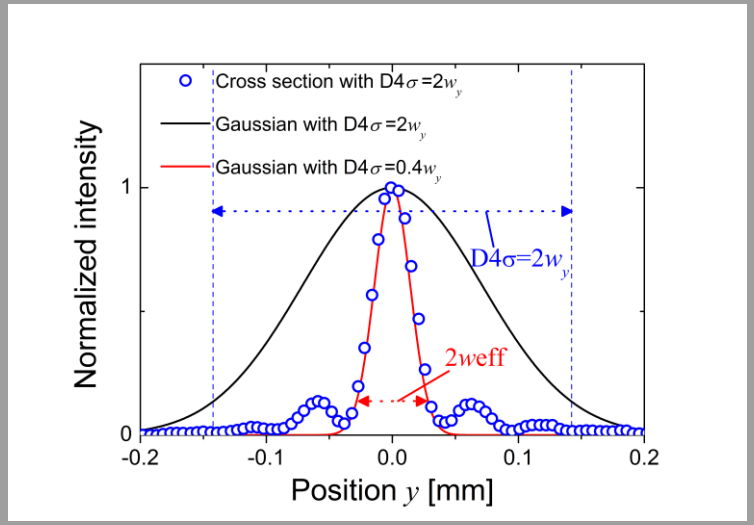

- The center part (red line) of Bessel-like beam has 0.2 times smaller size than $D4\sigma$ (black line).
- The small center part can increase focusability substantially.

$$M^2_{eff} = \frac{\pi w_{0,eff}}{\lambda}\theta = \frac{\pi w_{0,eff}}{\lambda} \cdot \frac{\lambda M^2}{\pi w_0} = \frac{w_{0,eff}}{w_0} M^2 = 0.2 \times 6 = 1.2.$$

M^2_{eff}: effective M^2

$w_{0,eff}$: effective beam waist

θ: half angle divergence

H. H. Lim and T. Taira, Opt. Express **27**, 31307 (2019).

Laser characteristics around far-field

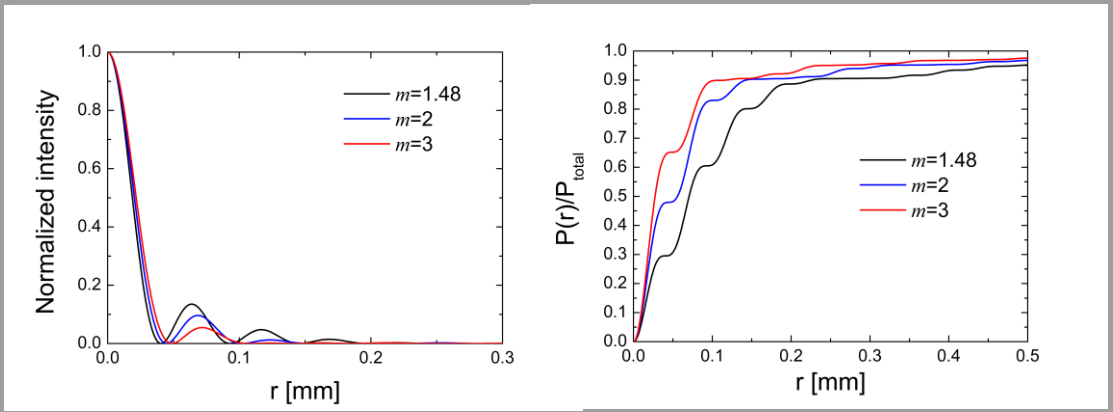

►The center part portion of pulse energy

$E_{eff} \approx 30\%$ for m=1.48

$E_{eff} \approx 65\%$ for m=3

Intensity distribution of plane wave focused by an annular aperture at the focal plane

$$I(r,f) = \frac{4\,I(0,f)}{(1-1/m^2)^2}\left[\frac{J_1(kr\,b/f)}{kr\,b/f} - \frac{1}{m^2}\frac{J_1(kr\,a/f)}{kr\,a/f}\right]^2, \qquad (1)$$

where $m = b/a$ is the ratio of the outer radius b and the inner radius a of the aperture, $S = \pi a^2(m^2-1)$ is the annular area, J_1 is the first-order Bessel function, $k = 2\pi/\lambda$ is the wave number, f is the focal length, and $I(0,f) = S^2/(\lambda^2 f^2)$ is the peak intensity at the focal plane. [1] B. Lu, et al., J. Mod. Opt. **48**, 1171 (2001).

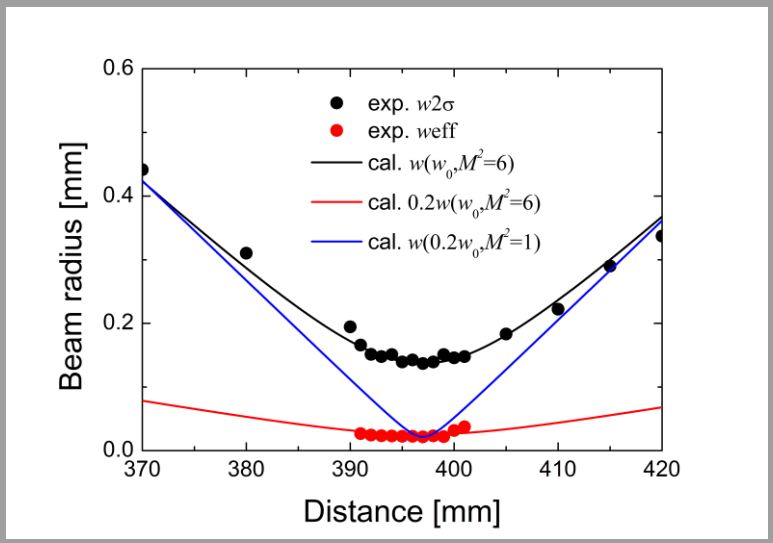

►The center part self-diffracts as the same as $D4\sigma$

►The effective Rayleigh length of the center part is about 4 times longer than that of Gaussian. $z_{R,eff} \approx 4 \times z_{R,G(M^2=1)}$

(Red line) (Blue line)

H. H. Lim and T. Taira, Opt. Express **27**, 31307 (2019).

Compared brightness to other works

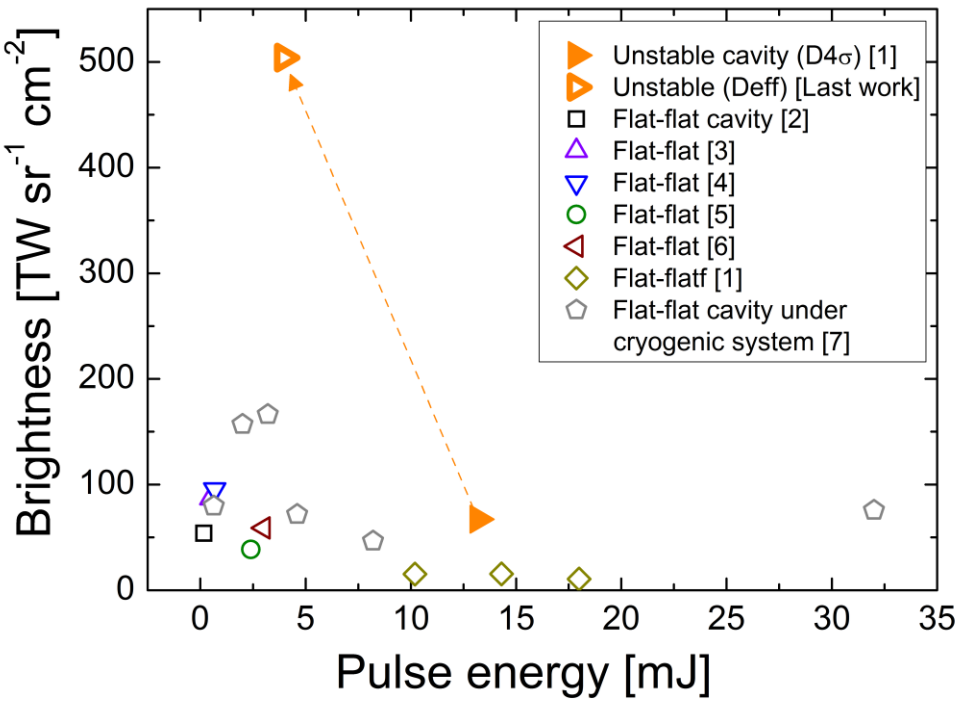

[1] H. H. Lim and T. Taira, Opt. Express **27**, 31307 (2019).

[2] J. Dong, et al., Opt. Express **15**, 14516 (2007).

[3] A. Agnesi, et al., Appl. Phys. Lett. **89**, 101120 (2006).

[4] H. Sakai, T. Taira, et al., Opt. Express **16**, 19891 (2008).

[5] N. Pavel, T. Taira, et al., Opt. Express **19**, 9378 (2011).

[6] H. H. Lim and T. Taira, Opt. Express **25**, 6302 (2017).

[7] X. Guo, et al., Opt. Express **27**, 45 (2019).

- $E_{eff} = 30\%,\ \ M_{eff}^2 = 1.2$
- Highest effective brightness of over 0.5 PW sr^{-1} cm^{-2}

Laser induced breakdown (LIB) in air

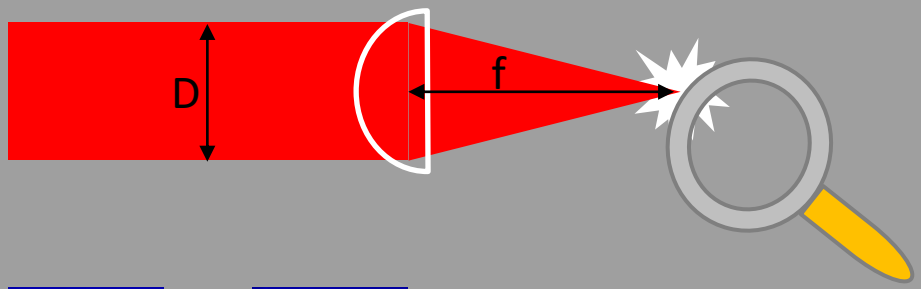

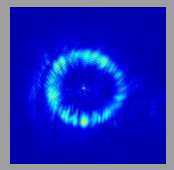

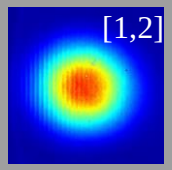

D=7.5 mm
τ=0.57 ns
M^2= 5.1

D=7.5 mm
τ=0.57 ns
M^2=1.3

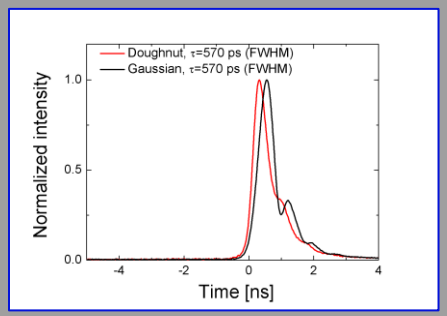

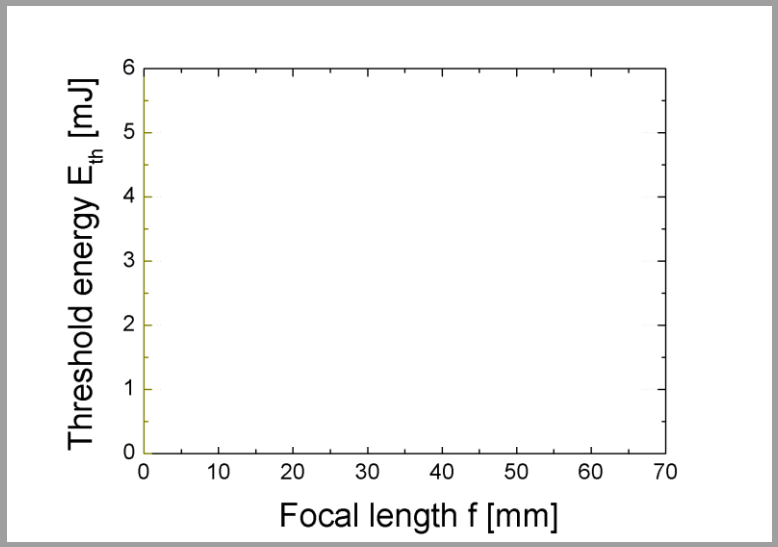

- Comparable capability of LIB to a near-Gaussian beam due to the effective high brightness of doughnut beam at focal plane

[1] H. H. Lim and T. Taira, Opt. Express **25**, 6320 (2017).
[2] H. H. Lim and T. Taira, Opt. Express **27**, 31307 (2019).

Experimental setup II : flat-convex cavity & uniform pump-power distribution

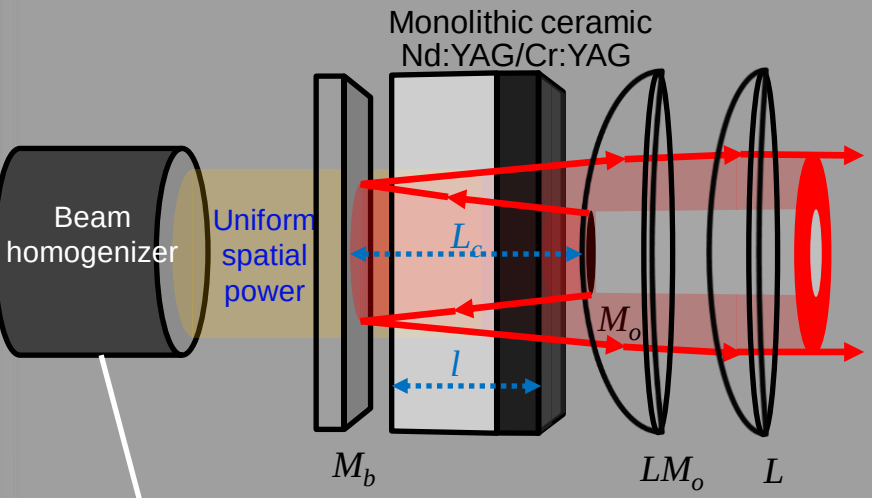

- 1.5 kW pump diode @ 808 nm, 20 Hz during <400 μs
- Uniform pump power distribution: ~3 x 3 mm^2

- Flat back cavity mirror M_b
- A half inch plano-convex lens LM_0 with a radius of curvature of 52 mm (for m of $\sqrt{2}$ for the confocal cavity)
- Output coupler (OC) M_0, HR coated on the center part of LM_0 in a spot diameter of 2 mm
- Collimation lens L with a focal length of 50~150 mm in case of the lens position

Experimental setup II : flat-convex cavity & uniform pump-power distribution

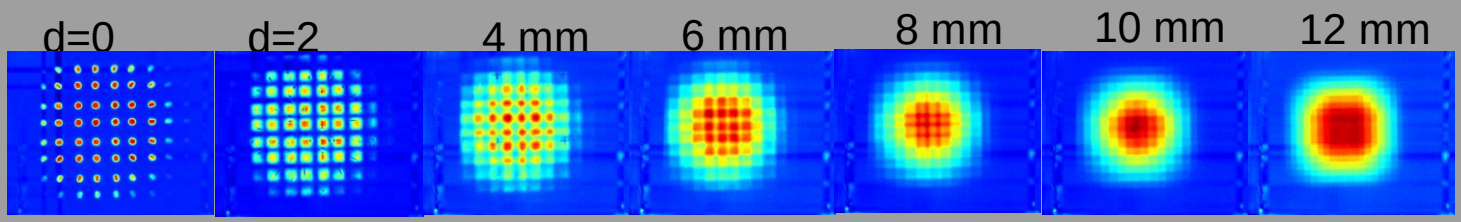

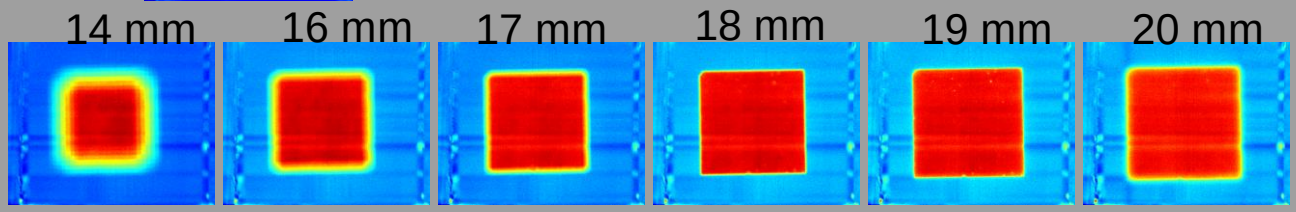

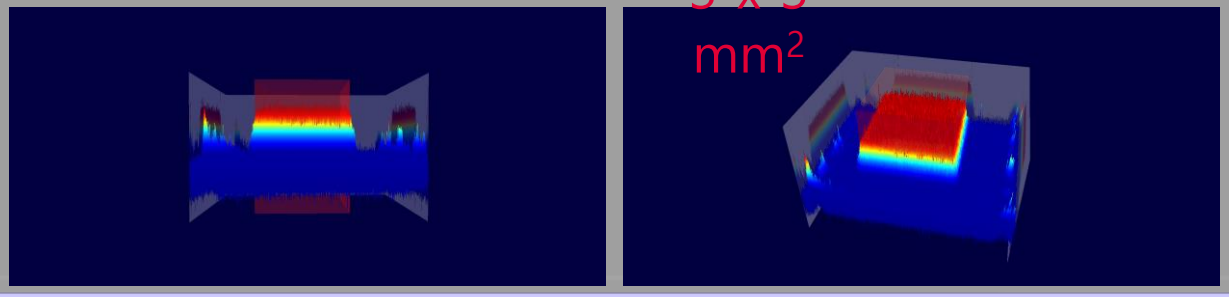

Results of set-up II

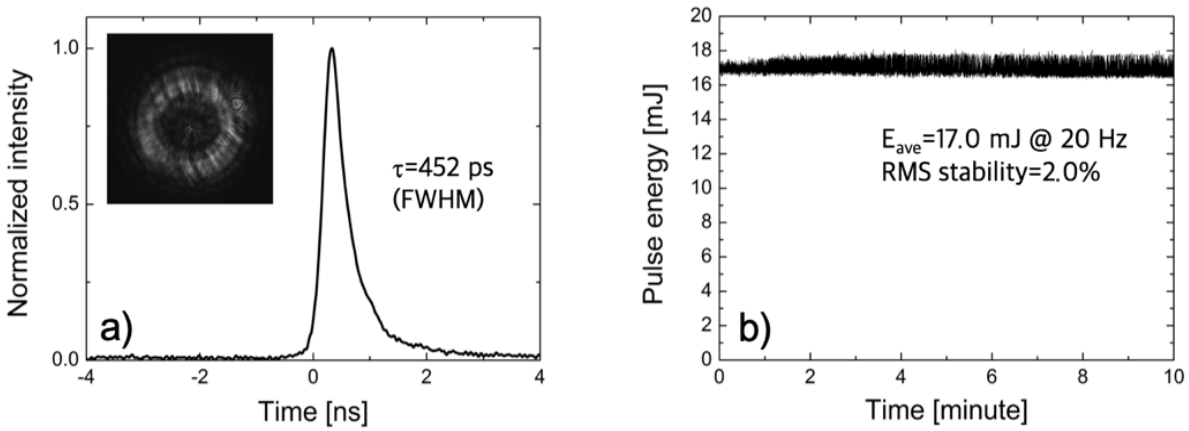

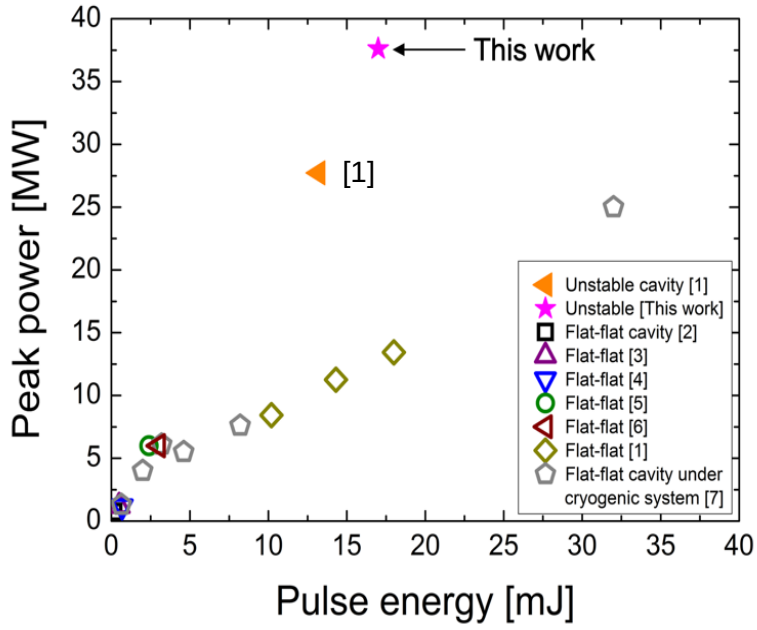

- Doughnut beam pattern
- Pulse energy of 17 mJ @ 20 Hz
- Pulse width of 452 ps
  - New record peak power of 37.6 MW

[1] H. H. Lim and T. Taira, Opt. Express **27**, 31307 (2019).

Experimental setup III : concave-convex cavity & uniform pump-power distribution

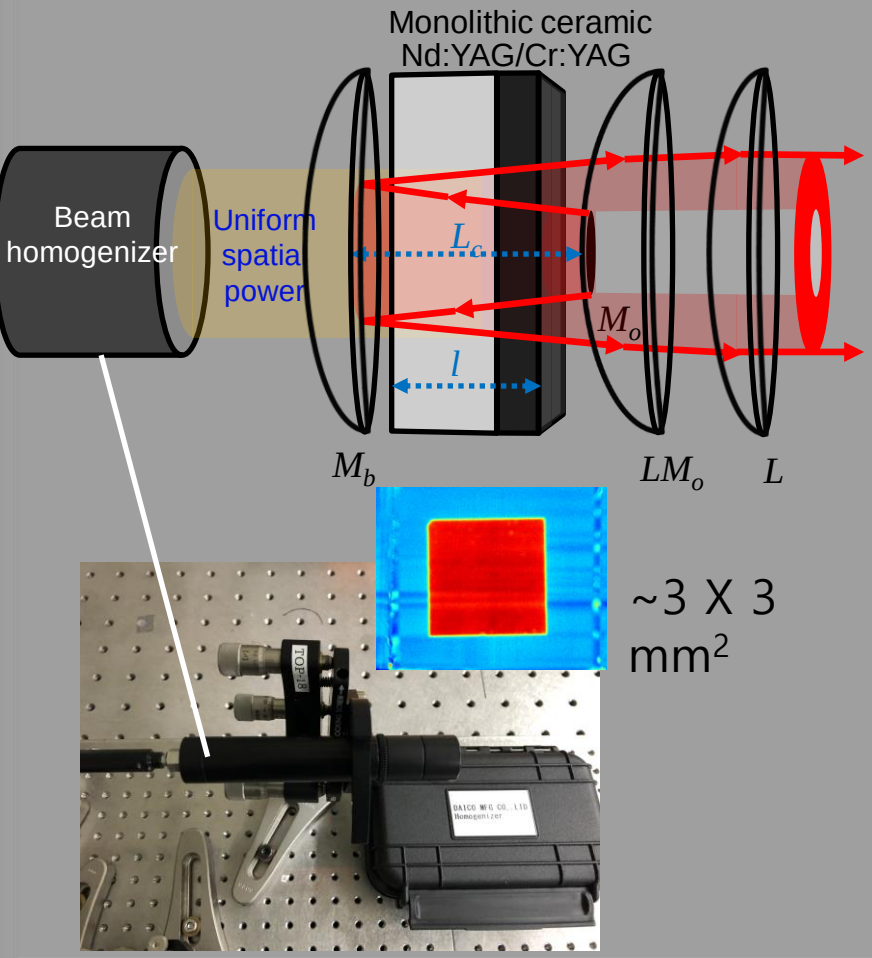

- 1.5 kW pump diode @ 808 nm, 20 Hz during <400 μs
- Uniform pump power distribution: ~3 x 3 mm²
- Concave back cavity mirror M_b with a radius of curvature of 250 mm
- A half inch plano-convex lens LM_0 with a radius of curvature of 52 mm (for m of $\sqrt{2}$ for the confocal cavity)
- Output coupler (OC) M_0, HR coated on the center part of LM_0 in a spot diameter of 2 mm
- Collimation lens L with a focal length of 50~150 mm in case of the lens position

Results of set-up III

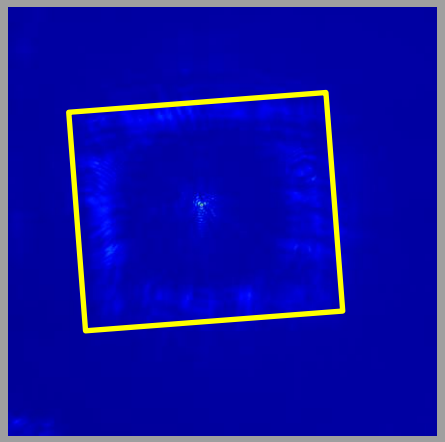

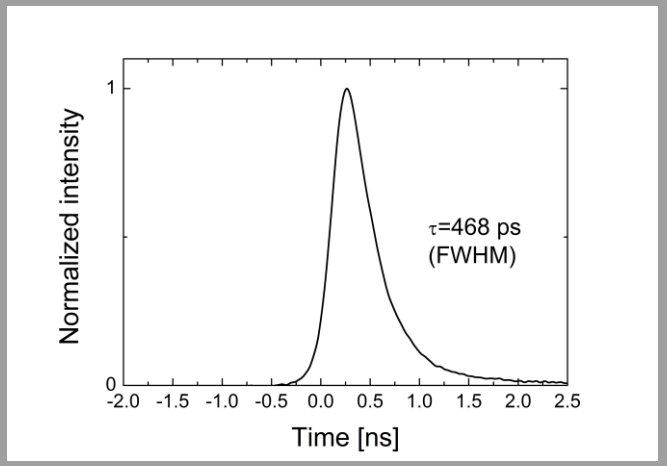

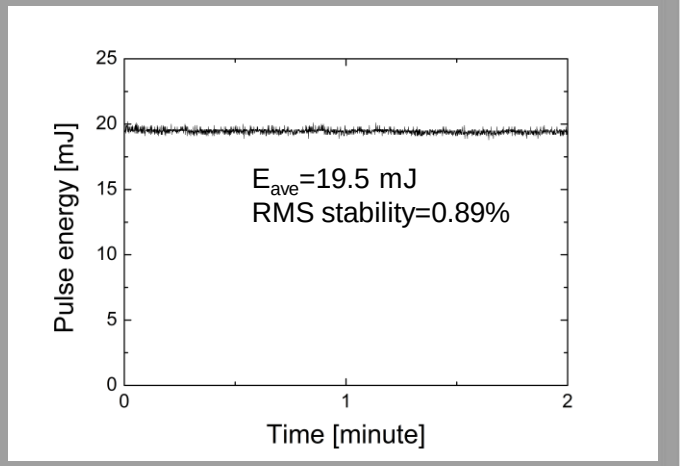

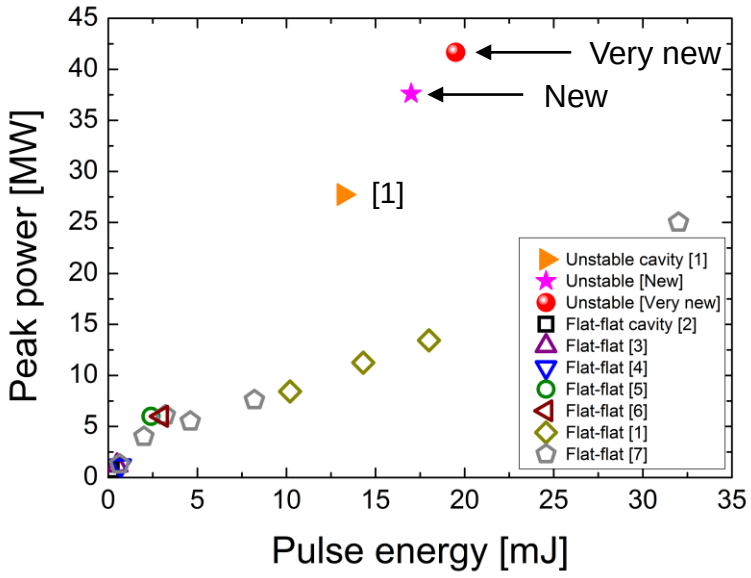

- Modified doughnut beam pattern
- Pulse energy of 19.5 mJ @ 20 Hz
- Pulse width of 452 ps
  - New record peak power of 41.7 MW

[1] H. H. Lim and T. Taira, Opt. Express **27**, 31307 (2019).

Summary

- Overview of fs laser micromachined waveguides

- Record peak power unstable cavity microchip laser:
  - 41.7 MW, 19.5 mJ, 468 ps

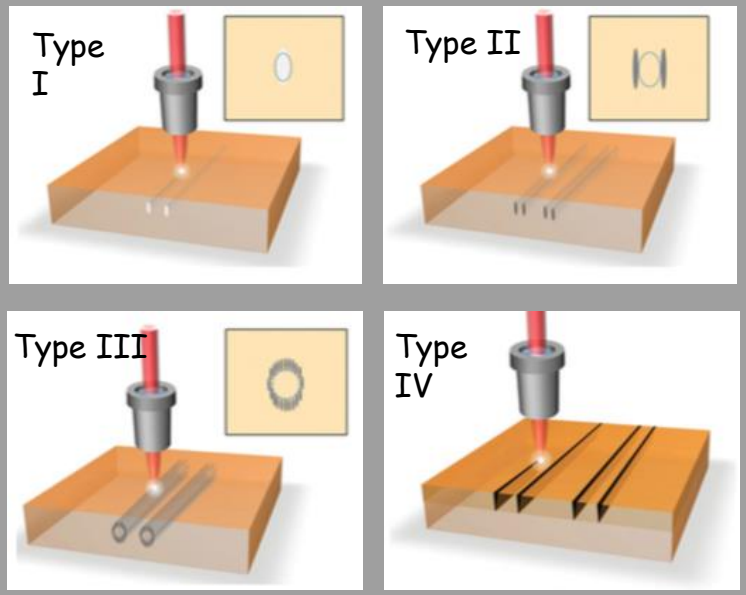

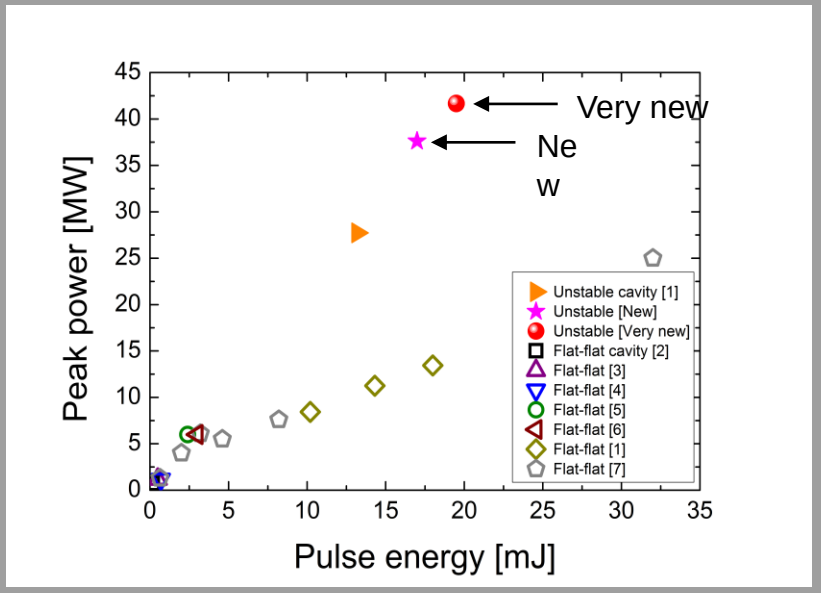

Future plan

- Laser writing system development (with Laser system Inc.).
- Test of unstable cavity MCL for laser writing (in laser and nonlinear materials such as Nd:YAG ceramics and crystals, LN, …), which may be compared with a reference using a fs-laser from Prof. Sugimoto group (< 1 mJ, 200 fs, 300 kHz) if possible.
- Further peak power and repetition rate scale of unstable cavity MCL using DFC chip.